Computational Sciences and Engineering 3(1) (2023) 1-10

University of Guilan

Computational Sciences and Engineering

journal homepage: https://cse.guilan.ac.ir/

The Modelling of Laser Parameters Effects on Temperature Changes in Different Tissues

Masoume Masoumipoor [a,b], Babak Babakhani [c], Seyed Behnamedin Jameie [d,e], Abbas Majdabadi [f], Mehdi Salehi Barough [a,b,*]

[a] Department of Medical Radiation Engineering, Central Tehran Branch, Islamic Azad University, Tehran, Iran

[b] Medical Radiation Research Center, Central Tehran Branch, Islamic Azad University, Tehran, Iran

[c] Department of Brain and Spinal Cord Injury Research Centre, Neuroscience Institute, Tehran University of Medical Sciences, Tehran, Iran

[d] Department of Anatomy, School of Medicine, Iran University of Medical Sciences, Tehran, Iran

[e] Neuroscience Research Center, Iran University of Medical Sciences, Tehran, Iran

[f] Department of Laser Research Center of Dentistry, Dentistry Research Institute, Tehran University of Medical Sciences, Tehran, Iran

ARTICLE INFO

Article history:
Received 4 February 2023
Received in revised form 25 February 2023
Accepted 26 February 2023
Available online 26 February 2023

Keywords:
Photobiomodulation
Thermal distribution
COMSOL Multiphysics

ABSTRACT

The present analysis estimated the changes of temperature subsequent laser therapy on skin, subcutaneous adipose tissues and muscle, by COMSOL Multiphysics software. Different thickness of tissues were selected and irradiated by continuous mode of wavelengths of laser with Gaussian beam profile. A preliminary model of combining the optical and thermal characteristics of these tissues was designed. The simulations predict the thermal distribution of laser on tissues corresponding to different wavelengths and different beam doses. The results of the data analysis indicated that laser irradiation at different wavelengths can increase skin temperature 37 up to 39 degrees of centigrade in photobiomodulation technique. The enhancement of temperature showed insignificant impact on subcutaneous adipose tissues and was negligible on the deep tissues such as muscle. The estimations could be validated by experimental trials.

1. Introduction

The biological effects of laser changes by the wavelength, power, the time profile of irradiation, tissue profile, and the physical properties of the material [1]. Photobiomodulation (PBM) employs

* Corresponding author.
E-mail addresses: m.s.barough@gmail.com (M. Salehi Barough)

https://doi.org/10.22124/cse.2023.23784.1046

an “optical window” from wavelengths of 600 nm to 1100 nm, with 1 to 20 J/cm^2 energy density of laser beam to heal various musculoskeletal damages [2-4]. In the therapeutic method, the photons absorbed by cellular photoreceptors were followed with activation of biochemical pathways [5-14]. Increases of temperature in the target tissue should be less than 1°C and the energy of laser is enough below the level of secure body temperature [15, 16]. Therefore, the effects of PBM is biochemical not thermal and absorbed light employs a chemical transformation [4]. In this way, understanding and predicting temperature progression during laser therapy becomes essential. Additionally, providing the beneficial simulations for growing efficacy by optimizing laser beam parameters is obligatory.

COMSOL Multiphysics, as a software, provides a user-friendly situation to investigate a wide range of physical occurrences [17]. Reviews of literatures have presented that COMSOL software is a potent instrument for creating more precise computation than other simulation methods of light and tissue interactions have shown its uniformity to provide essential information. [18].

The analysis of literature has shown COMSOL Multiphysics were utilized for assessing and plotting the accurate models to evaluate effective parameters in different laser therapy techniques [19-22].
The present study is to progress a computational model in order to assess the thermal distribution in the tissues during the LLLT irradiated with continuous wave of lasers with Gaussian profile. For this purpose, a 3D simulation COMSOL model which is a simple tool for designing a light source inducing photobiomodulation, was employed for computing the extent of heat in several tissues.

2. Materials and methods

2.1. Modeling process

The effects of different wavelengths of laser beams on different type of tissues were investigated. As it is mentioned before, COMSOL Multiphysics software was used to investigate the thermal effects of transferred energy to the tissues that modeling process shown in ***Fig. 1*** graphical abstract.

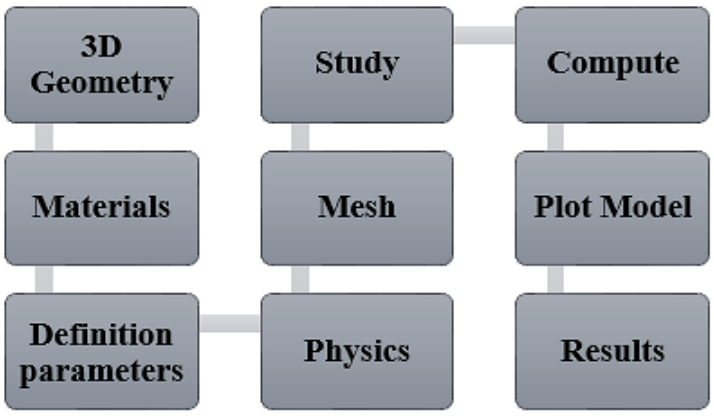

Figure 1. Graphic of modelling process

2.2. Tissue Modeling

2.2.1. Geometry of the model

A cube with 18 mm × 18 mm × 18 mm dimensions, consisting of different layers and diverse thicknesses created that including skin (type II), subcutaneous adipose tissue and muscle. Thickness assumed for tissue layers contains skin 3mm, subcutaneous adipose tissue 5mm and muscle 10mm [23].

2.2.2. Tissue optical properties

The diagnostic and therapeutic techniques are affected by tissue optical properties. The penetration depth of laser and deposited energy in tissues, extremely depend on tissue optical properties [24]. In this simulation optical properties of tissues were defined. Absorption coefficient μ_a (cm^{-1}) in ***Table 1*** and reduced scattering coefficient μ'_s (cm^{-1}) in ***Table 2*** were used. These coefficients were extracted from literatures for different wavelengths and tissues [25-31].

Table 1. Absorption coefficient μ_a (cm^{-1}) for different wavelengths and different tissues [26-28]

Wavelength (nm)	Skin	Adipose Tissue	Muscle
600	0.69	1.18	1.23
700	0.48	1.11	0.48
800	0.43	1.07	0.28
900	0.33	1.07	0.32
1000	0.27	1.06	0.51
1100	0.16	1.01	0.13

Table 2. Reduced scattering coefficient μ'_s (cm^{-1}) for different wavelengths and different tissues [26-28]

Wavelength (nm)	Skin	Adipose Tissue	Muscle
600	28.1	13.4	8.94
700	16.7	12.2	8.18
800	14.0	11.6	7.04
900	15.7	10.0	6.21
1000	16.8	9.39	5.73
1100	17.1	8.74	5.84

2.2.3. Tissue thermal properties

The thermal properties were affected by the amount of water in tissue [32]. Three essential thermal parameters of tissues which are used in the physics of the simulation include density, heat capacity and thermal conductivity in ***Table 3*** [33].

Table 3. Thermal properties of different tissues [33]

Thermal parameters	Skin	Adipose Tissue	Muscle
Density (kg/m^3)	1109	911	1090
Heat Capacity (J/(kg·K))	3391	2348	3421
Thermal Conductivity (W/m/°C)	0.37	0.21	0.49

2.3. Heat Source Modeling

The thermal distribution assessed by Beer-Lambert law [34]. The present simulation, the laser beam modeled as a heat source. The deposited energy through absorbed beam, considered as a heat source.

The heat transfer was explained by ***Eq. (1)***:

$$Q = \sum_i \kappa i \; I \tag{1}$$

Where,

κ_i is the summation of the absorption coefficient (cm^{-1}) and the reduced scattering coefficient (cm^{-1}) for any kind of tissue and I is the beam intensity (W/cm^2).

When the laser beam affects the tissues, metabolic heat is negligible in comparison with external heat that is induced by laser. The heat extraction by blood circulation considers by Pennes equation ***Eq. (2***) [36].

$$\rho C_p \frac{\partial T}{\partial t} + \nabla . q = \rho_b C_{p.b} \omega_b (T_b - T) + Q_{met} \tag{2}$$

The power of laser beam as a heat source was considered 500 mw that is the highest power of low-level laser beams [36]. The energy densities as a dose of laser beam was considered zero up to 20 J/cm^2. To achieve these values, the laser radiation time was calculated zero up to 40 seconds. The distance between beam origin and tissue surface was assumed as 3cm.

With the purpose of defining the thermal development, the bio-heat transfer application mode and time dependent study by means of series (0, 0.2, 40) seconds were employed. The initial temperature of tissues was considered T_0=37°C.

3. Results

Overall, by using this modeling at any depth of tissues and at any point of time, the thermal distribution could be estimated.

Graphs evince temperature changes at various times and diverse tissues. Regarding the values, alteration of temperature could be clinically important. As it is presented, after spending 30 seconds, changes of temperature are very slight. Through the time and energy density increases, the temperature rises.

The highest temperatures occurred at the skin level in the wavelength of 600nm and 700 nm, after spending 40 seconds in the energy of 20 J/cm^2 the temperature reaches about 39 ℃ in ***Figs. (2) & (3)***.

The lowest temperature was run in the wavelength of 800nm, after 40 seconds the temperature reaches 38.4℃ at the skin surface in ***Fig. 4***. Furthermore, the temperature was observed about 38.7℃ at the other wavelengths. Following increasing depth in tissues, the temperature is reduced and reaches less than 37.5℃ at subcutaneous tissues in ***Figs. (5) - (7)***.

According to the outcomes of the modeling, increasing the temperature in tissues is dependent on coefficients of tissues in the certain wavelength and beam doses. As expected, with the assessment of PMB parameters, enhancement of temperature is not tangible and deleterious.

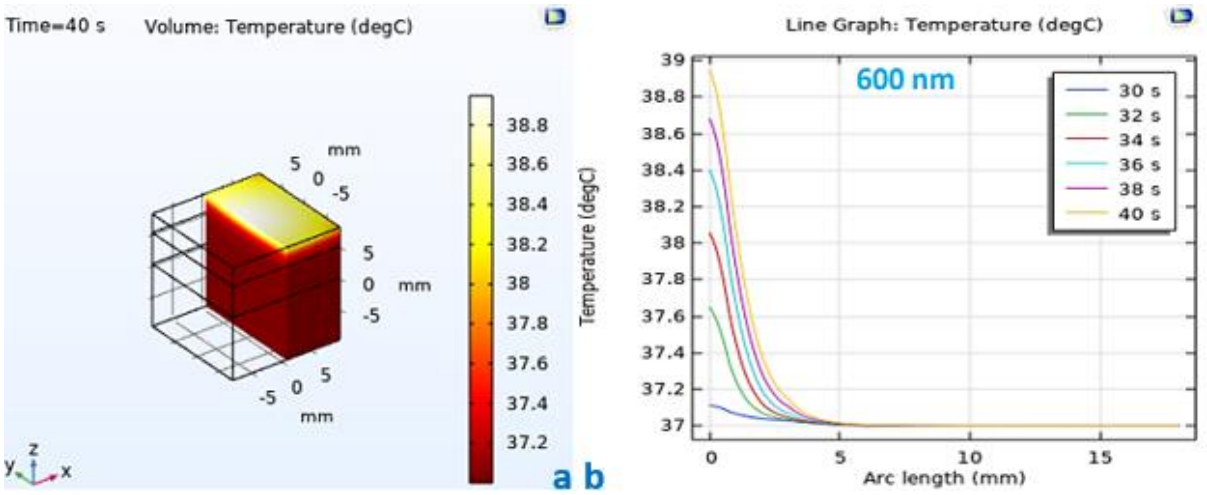

Figure 2. (a) 3D schematic of the temperature distribution in entire geometry, after 40 seconds in wavelength of 600 nm. (b) Line graph of the temperature distribution at several times and in different depth of sample, in wavelength of 600 nm.

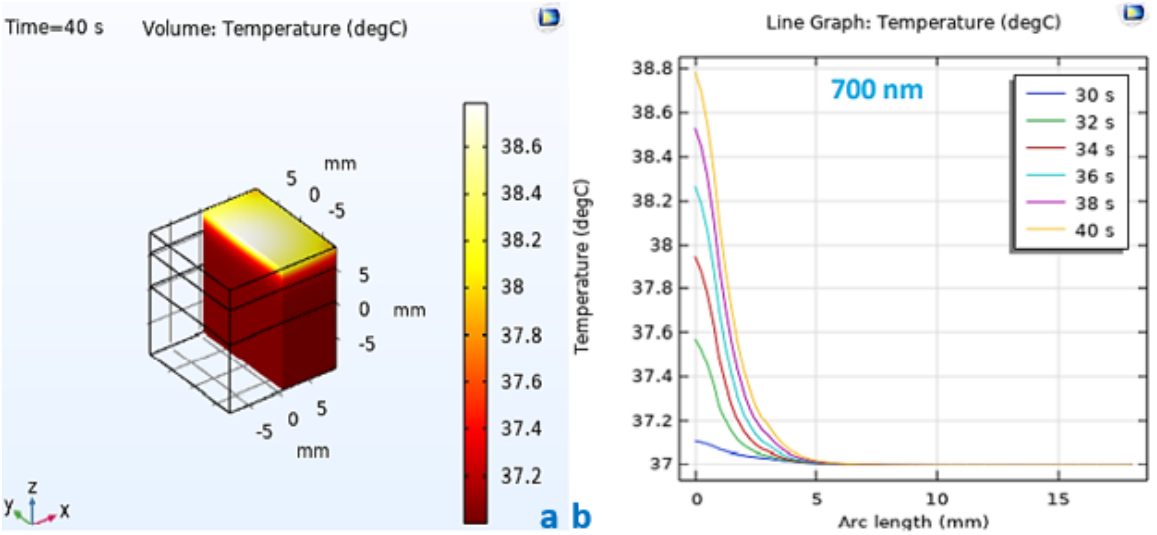

Figure 3. (a) 3D schematic of the temperature distribution in entire geometry, after 40 seconds in wavelength of 700 nm. (b) Line graph of the temperature distribution at several times and in different depth of sample, in wavelength of 700 nm.

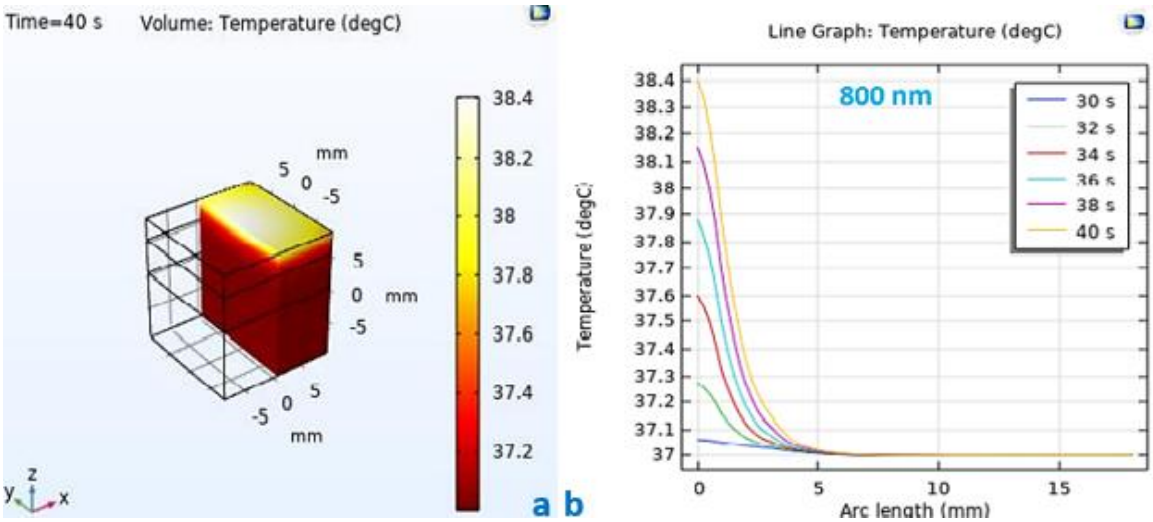

Figure 4. (a) 3D schematic of the temperature distribution in entire geometry, after 40 seconds in wavelength of 800 nm. (b) Line graph of the temperature distribution at several times and in different depth of sample, in wavelength of 800 nm.

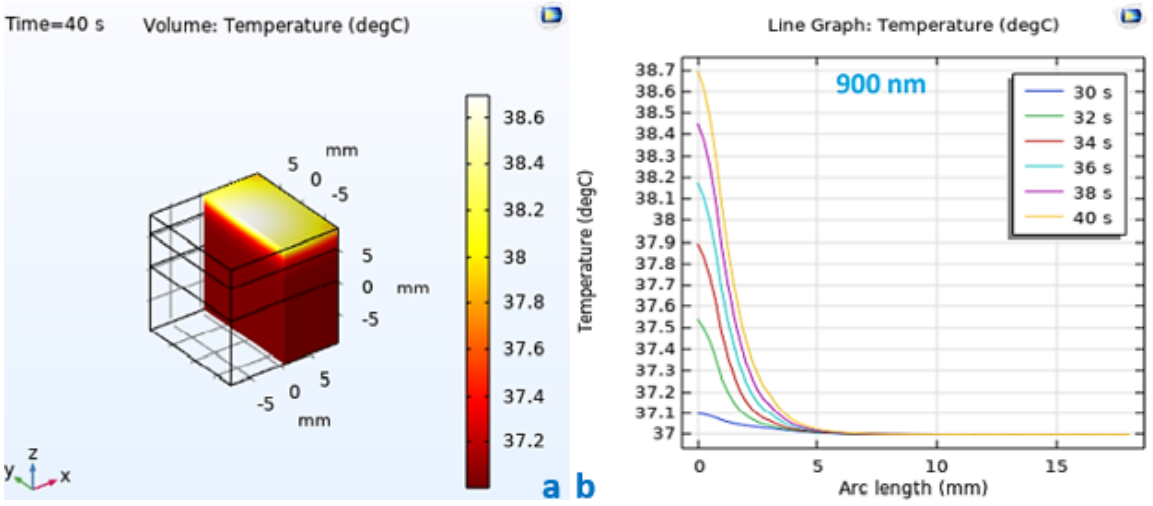

Figure 5. (a) 3D schematic of the temperature distribution in entire geometry, after 40 seconds in wavelength of 900 nm. (b) Line graph of the temperature distribution at several times and in different depth of sample, in wavelength of 900 nm.

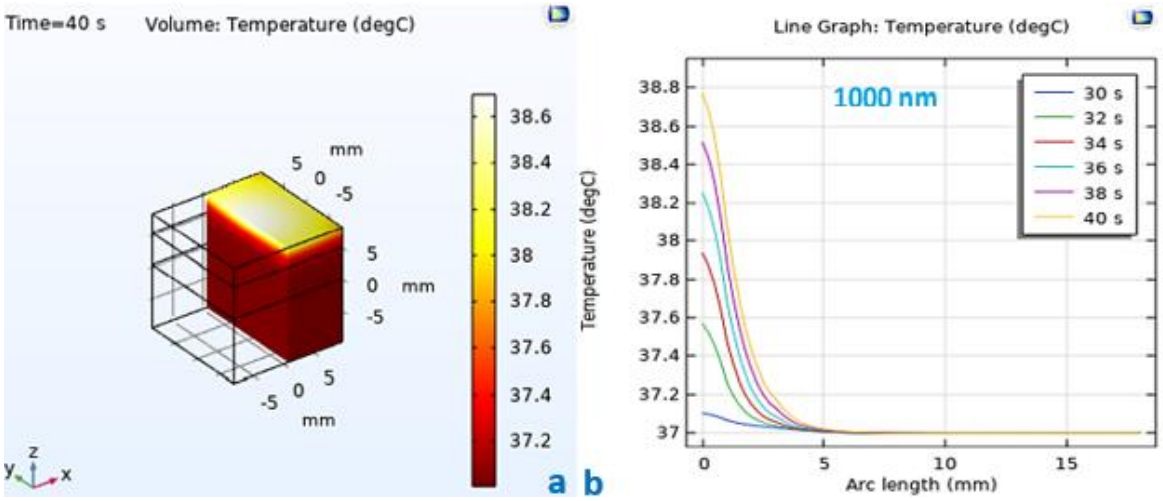

Figure 6. (a) 3D schematic of the temperature distribution in entire geometry, after 40 seconds in wavelength of 1000 nm. (b) Line graph of the temperature distribution at several times and in different depth of sample, in wavelength of 1000 nm.

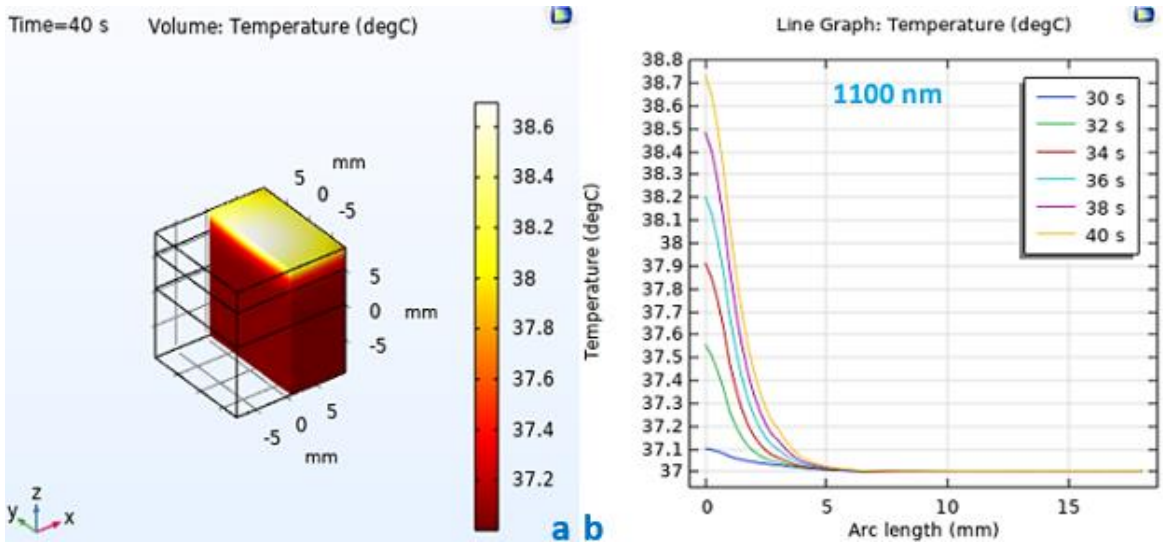

Figure 7. (a) 3D schematic of the temperature distribution in entire geometry, after 40 seconds in wavelength of 1100 nm. (b) Line graph of the temperature distribution at several times and in different depth of sample, in wavelength of 1100 nm.

4. Discussion

The survey of simulations represents complex mathematical or simple solutions [32, 37], although there is a lack of study about the prediction of tissue damages, oriented to the clinical application. Modelling of heat deposition in tissues for laser and tissue interactions were suggested based on the reduced scattering coefficient (μ'_s) and absorption coefficient μ_a). Furthermore, the reaction determination of temperature was simulated by the heat conduction equation [38].

In the present model, coefficients were used to estimate thermal distribution and heat deposition. COMSOLMultiphysics 5.6a was employed to evaluate laser parameters and the time of treatment with the purpose of a new conception for photobiomodulation.

Biological phenomena occur at different temperatures during the photo-thermal therapy. Biological effects were considered as bio stimulation at <43°C, hyperthermia at 43-45°C, reduction in enzyme activity at 50°C and protein denaturation (coagulation) at 60°C. Therefore, to achieve photobiomodulation occurrences, the temperature changes in biological tissues should be up to 43°C. Higher temperatures can motive harmful thermal effects on the tissues [39-42].

The preliminary outcomes will be suitable when planning the experimental studies to induce optimal values without damage and the temperature changes.

In the present modeling, it is revealed that continuous radiation of laser for 40 seconds with 500mw power can not damage the tissues due to increased temperature; hence to prevent damage, it may be crucial to limit the time of radiation bellow 40 seconds. Higher beam doses with higher powers lead to higher temperatures at irradiated tissues that prevent PBM phenomena. In the case of direct contact with skin, increases of temperature could be more significant than non-contact state.

Further studies of different parameters of laser therapy can lead to developing an application Based on model designing.

5. Conclusion

COMSOL Multiphysics software was utilized to plan initial assessments and a device optimization for selective treatment. This model could be used as a support tool in laser therapy devices to obtain more safe protocols for both animal and human subjects. Furthermore, the practice with this computer-based technology enables us to reduce the number of animals in experiments and preclinical research.

References

[1] Mohammed, Y., & Verhey, J. F. (2005). A finite element method model to simulate laser interstitial thermo therapy in anatomical inhomogeneous regions. *Biomed Eng Online*, 4(2), 1-16.
[2] Karu, T. I., & Afanas'eva, N. I. (1995). Cytochrome c oxidase as the primary photoacceptor upon laser exposure of cultured cells to visible and near IR-range light. *Dokl Akad Nauk* , 342(5), 693-695.
[3] Karu, T. I., & Kolyakov, S. F. (2005). Exact action spectra for cellular responses relevant to phototherapy. *Photomed Laser Surg*, 23(4), 355-361.
[4] Huang, Y. Y., Sharma, S. K., Carroll, J., & Hamblin, M. R. (2011). Biphasic Dose Response in Low Level Light Therapy – *An Update. Dose-Response*, 9(4), 602–618.
[5] Passarella, S., Casamassima, E., Molinari, S., Pastore, D., Quagliariello, E., Catalano, I. M., & Cingolani, A. (1984). Increase of proton electrochemical potential and ATP synthesis in rat liver mitochondria irradiated in vitro by helium-neon laser. *FEBS Lett*, 175(1), 95-99.
[6] Borutaite, V., Budriunaite, A., & Brown, G. C. (2000). Reversal of nitric oxide-, peroxynitrite- and Snitrosothiol-induced inhibition of mitochondrial respiration or complex I activity by light and thiols. *Biochimica ET biophysica acta*, 1459(2-3), 405-412.
[7] Sutherland, J. C. (2002). Biological effects of polychromatic light. *Photochem Photobiol*, 76(2), 164-170.
[8] Lubart, R., Eichler, M., Lavi, R., Friedman, H., & Shainberg, A. (2005). Low-energy laser irradiation promotes cellular redox activity. *Photomed Laser Surg*, 23(1), 3-9.
[9] Lane, N. (2006). Cell biology: power games. *Nature*, 443(7114), 901-903.
[10] Shiva, S., & Gladwin, M. T. (2009). Shining a light on tissue NO stores: near infrared release of NO from nitrite and nitrosylated hemes. *J Mol Cell Cardiol*, 46(1), 1-3.

[11] Lohr, N. L., Keszler, A., Pratt, P., Bienengraber, M., Warltier, D. C., & Hogg, N. (2009). Enhancement of nitric oxide release from nitrosyl hemoglobin and nitrosyl myoglobin by red/near infrared radiation: Potential role in cardioprotection. *J Mol Cell Cardiol*, 47(2), 256–263.

[12] Zhang, R., Mio, Y., Pratt, P. F., Lohr, N., Warltier, D. C., Whelan, H. T., Zhu, D., Jacobs, E. R., Medhora, M., & Bienengraeber, M. (2009). Near infrared light protects cardiomyocytes from hypoxia and reoxygenation injury by a nitric oxide dependent mechanism. *J Mol Cell Cardiol*, 46(1), 4-1.

[13] Ball, K. A., Castello, P. R., Poyton, R. O. (2011). Low intensity light stimulates nitrite-dependent nitric oxide synthesis but not oxygen consumption by cytochrome c oxidase: Implications for phototherapy. *J Photochem Photobiol B*, 102(3), 182-191.

[14] Poyton, R. O., & Ball, K. A. (2011). Therapeutic photobiomodulation: nitric oxide and a novel function of mitochondrial cytochrome c oxidase. *Discov Med*, 11(57), 154-159.

[15] Hrnjak, M., Kuljic- kapulica, N., Budisin, A., & Giser, A. (1995). Stimulatory effect of low-power density He-Ne laser radiation on human fibroblast in vitro. *Vojnosanit Pregl*, 52(6), 539-546.

[16] Lim, H. M., Lew, K. K., & Tay, D. K. (1995). A clinical investigation of the efficacy of low-level laser therapy in reducing orthodontic postadjustment pain. *Am J Orthod Dentofacial Orthop*, 108(6), 614-622.

[17] Yang, L., Wei, T., Lisheng, L., Junfeng, S., Ming, S., & Xiangzheng, C. (2020). Study on Heat Effect of High-Power Continuous Wave Laser on Steel Cylinder. *Appl. Sci*, 10(21), 7844.

[18] Kirmani, S. A. M., Velmanickam, L., Nawarathna, D., Sherif, S. S., & Jr, I. T. L. (2016). Simulation of Diffuse Optical Tomography Using COMSOL Multiphysics. *Proc. COMSOL Conf. Bost*.

[19] Marqa, M. F., Colin, P., Nevoux, P., Mordon, S., & Betrouni, N. (2010). Laser Interstitial Thermo Therapy (LITT) for Prostate Cancer Animal Model: Numerical Simulation of Temperature and Damage Distribution. *Proc. COMSOL Conf. Paris*.

[20] Rossi, F., Ratto, F., & Pini, R. (2012). Laser Activated Gold Nanorods for the Photothermal Treatment of Cancer. *Proc. COMSOL Conf. Milan*.

[21] Nour, M., Lakhssassi, A., Kengne, E., & Bougataya, M. (2015). 3D Simulation of the Laser Interstitial Thermal Therapy in Treatment (LITT) of Brain Tumors. *Proc. COMSOL Conf. Bost*.

[22] Manrique-Bedoya, S., Moreau, C., Patel, S., Feng, Y., & Mayer, K. (2019). Computational Modeling of Nanoparticle Heating for Treatment Planning of Plasmonic Photothermal Therapy in Pancreatic Cancer. *Proc. COMSOL Conf. Bost*.

[23] Neumann, E. E., Owings, T. M., Schimmoeller, T., Nagle, T. F., Colbrunn, R. W., Landis, B., Jelovsek, J. E., Wong, M., Ku, J. P., & Erdemir, A. (2018). Reference data on thickness and mechanics of tissue layers and anthropometry of musculoskeletal extremities. 5:180193 DOI: 10.1038/sdata.2018.193.

[24] Jacques, S. L. (2013). Optical properties of biological tissues: a review. *Phys. Med. Biol*, 58(11), 37–61.

[25] Cheong, W. F. (1995). Appendix to chapter 8: Summary of optical properties Optical-Thermal Response of Laser Irradiated Tissue. 1st edn ed A J Welch and M J C van Gemert (New York: Plenum)

[26] Bashkatov, A. N., Genina, E. A., Kochubey, V. I., & Tuchin, V. V. (2005). Optical properties of human skin, subcutaneous and mucous tissues in the wavelength range from 400 to 2000 nm. *J. Phys. D: Appl. Phys*, 38(15), 2543-2555.

[27] Bashkatov, A. N., Genina, E, A., Kochubey, V. I., & Tuchin, V. V. (2005). Optical properties of the subcutaneous adipose tissue in the spectral range 400-2500 nm. *Opt. Spectrosc*, 99(5), 836-842.

[28] Bashkatov, A. N., Genina, E. A., Kochubey, V. I., & Tuchin, V. V. (2011). Optical properties of skin, subcutaneous, and muscle tissues: a review. *J. Innov. Opt. Health Sci*, 4(1), 9–38.

[29] Sandell, J. L., & Zhu, T. C. (2011). a review of in-vivo optical properties of human tissues and its impact on PDT. *J. Biophotonics*, 4(11-12), 773–787.

[30] Welch, A. J., & van Gemert, M. J. C. (2011). Overview of optical and thermal laser-tissue interaction and nomenclature Optical-Thermal Response of Laser-Irradiated Tissue. 2nd edn ed A J Welch and M J C van Gemert (Berlin: Springer) chapter 1 (DOI: 10.1007/978-90-481-8831-4).

[31] Yi, J., & Backman, V. (2012). Imaging a full set of optical scattering properties of biological tissues by inverse spectroscopic optical coherence tomography *Opt. Lett*, 37(21), 4443–4445.

[32] Dua, R., & Chakraborty, S. (2005). A novelmodeling and simulation technique of photo -thermal interactions between lasers and living biological tissues undergoing multiple changes in phase. *Computers in biology and medicine*, 35(5), 447–462.

[33] Hasgall, P. A., Di Gennaro, F., Baumgartner, C., Neufeld, E., Lioyd, B., Gosselin, M. C., Payne, D., Klingenbock, A., & Kuster, N. 2022 IT'IS Database for thermal and electromagnetic parameters of biological tissues. Version 4.1, Feb 22, 2022, DOI: 10.13099/VIP21000-04-1.
[34] Welch, A. J., Pearce, J. A., Diller, K, R., Yoon, G., & Cheong, W, F. (1989). Heat generation in laser irradiated tissue. *Journal of biomechanical engineering*, 111(1), 62–68.
[35] Hamblin, M. R. (2016). Photobiomodulation or low-level laser therapy. *Journal of Biophotonics,* **9** (11–12), 1122–1124.
[36] Dewan, N., Kumar, A., & Attri, I. (2017). Optimization of laser parameters for studying the temperature profiles in the tissue. *International Journal of Advanced Technology in Engineering and science*, 5(1), 297-307.
[37] Jacques, S. L., & Prahl, S. A. (1987) Modeling optical and thermal distributions in tissue during laser irradiation. *Lasers in surgery and medicine*, 6(6), 494–503.
[38] Welch, A. J. (1985). Laser Irradiation of Tissue, In A. Shitzer and R. C. Eberhart (eds.), *Heat Transfer in Medicine and Biology*, pp. 135–184.
[39] Yoon, G. W. (1984). the thermal effect of laser beam scattering in biological medium. University of Texas at Austin.
[40] Brugmans, M. J., Kemper, J., Gijsbers, G. H., van der Meulen, F. W., & van Gemert, M. J. (1991). Temperature response of biological materials to pulsed non-ablative CO2 laser irradiation. *Lasers in surgery and medicine*, 11(6), 587–594.
[41] Miserendino, L. J., Levy, G. C., & Rizoiu, I. M. (1995). Effects of Nd:YAG laser on the permeability of root canal wall dentin. *Journal of Endodontics*, 21(2), 83–87.
[42] Banerjee, A., Ogale, A. A., Das, C., Mitra, K., & Subramanian, C. (2005) Temperature Distribution in Different Materials Due to Short Pulse Laser Irradaition. Heat Transfer Engineering, 26(8), 41-49.